

Application of Geometric Simulation for Determination of Dynamic Undeformed Chip Thickness in Milling

Sebastian Bombiński¹, Krzysztof Jemielniak^{2*}

¹ Kazimierz Pulaski University of Technology and Humanities in Radom, ul. Stasieckiego 54, 26-600 Radom, Poland

² Warsaw University of Technology, ul. Narbutta 86, 02-524 Warsaw, Poland

* Corresponding author's e-mail: krzysztof.jemielniak@pw.edu.pl

ABSTRACT

Self-excited vibration is a significant constraint on productivity and production quality, which makes various forms of virtual machining widely used to find stable conditions before starting the actual machining operation. Numerical simulation of self-excited vibration, although much slower than analytical solutions, makes it possible to consider the nonlinearity of the process and its continuous variation. In 5-axis milling, predicting the instantaneous cross-sections of the uncut chip is very difficult, so geometric simulation is readily used to check the correctness of the NC program and the obtained shape of the workpiece. However, the known solutions take into consideration only programmed movements of the tool relative to the workpiece without considering vibrations, and those in which attempts have been made to consider vibrations have significant limitations. This paper uses a Geometric Simulator that determines the nominal positions of the tool relative to the workpiece, to which the displacements due to vibration, determined by the Dynamic Simulator, are added, making it possible to effectively determine the dynamic thickness of the cut layer and the trace on the workpiece material left by the vibrating tool. The use of geometric simulation, in which the material is represented by discrete voxels, introduces signal quantization, that is, the limited resolution of undeformed chip thickness and trace left on the machined surface. The paper presents the effect of voxel dimension on the accuracy of the simulation of self-excited vibrations

Keywords: self-excited vibration, numerical simulation, computer graphics, 5-axis milling.

INTRODUCTION

Self-excited vibrations occurring in the cutting process are a major constraint on production efficiency, geometric and dimensional accuracy of machined parts, tool life, and machine tool durability. Hence the need to estimate a stability limit that allows the selection of chatter-free conditions before actual machining. In general, there are two methods for stability analysis: solving the differential equations of the system in the frequency domain or numerical simulation in the time domain [1, 2]. Quick and easy calculations in the frequency domain based on differential equations are possible using a simplified linear model of the cutting process. Despite the convenience of analytical calculation of the stability limit, the

main disadvantage of these methods is the inability (or considerable difficulty) to consider changes in the dynamic characteristics of the mass-spring-damper (MSD) system and cutting process (CP) in space and time. Numerical simulation in the time domain does not have these limitations [3, 4, 5]. It consists in determining, at short intervals dt , the instantaneous (variable) cross sections of the uncut chip and, on this basis, calculating the instantaneous cutting forces. The values of the forces are transferred to the next iteration, in which the deflections (vibrations) of the tool with respect to the workpiece caused by these cutting forces are determined based on the dynamic characteristics of the MSD system. This allows the calculation of the next uncut chip cross section that takes into consideration the vibrations.

Unfortunately predicting instantaneous cutting parameters in 5-axis milling is very difficult if not impossible. In addition, NC programs that contain machine control commands are not always error-free. Therefore, virtual machining using computer graphics for verification of milling operations has been widely implemented in the industry. The geometric removal of material on a machine tool is simulated graphically to verify the absence of collisions and the kinematic correctness of the tool path. There are several methods for identifying the conditions of tool-workpiece engagement along the tool path. In 5-axis free-form machining, dixel- or voxel-based systems are often used to model three-dimensional workpieces, while the tool is modeled by its envelope [6, 7]. The material removal process can be simulated using a time or displacement discretization of the tool path (Figure 1a, b), and the shape of the removed material can be easily and accurately determined using Boolean operations (Figure 1c).

Some publications go further, trying to predict not only the shape of the workpiece, but also the instantaneous cutting forces. E.g., Yousefian et al. [8] or Xi [9] proposed determining the cutting forces acting on individual edges resulting from nominal values of the chip thickness. The calculations do not consider dynamic changes in the chip thickness, so they cannot be used to simulate vibrations.

Nishida et al. [10] proposed a method for calculating the removed voxels in discrete intervals of the tool's rotation angle, as shown in Figure 2a. The tool is divided into disks perpendicular to the tool axis, and the removal of voxels is done by detecting those that lie in each disk, as shown in Figure 2b. This allows to calculate the cutting force acting on each disc, and then calculate the total cutting force acting on the cutter by adding up the cutting forces of all disc

components. The method applies to the simple case of end milling operation, hence cannot be applied to 5-axis milling.

Recently, Li et al. [11] presented a general model of the cutting dynamics of the 5-axis milling process with a ball mill, however, the dynamic thickness of the cut layer is determined analytically. For complex 5-axis milling, it is practically impossible to analytically determine the instantaneous uncut chip cross-section (b , h_d). Denkena et al. [12, 13] proposed determining the dynamic uncut thickness based on dexels. The simulation consists of calculating the intersections between the dixel lines and the rake face discretized with quadrilaterals (Figure 3a). The method was used for serrated milling cutters with circular indexable inserts (Figure 3b). In 5-axis milling, the rake surface may be temporarily parallel to the axis of symmetry, which would make it impossible to use this method.

In the CYBERTECH 4 intelligent process planning system SAPP (Smart Aided Process Planning) for Platform 4.0, a methodology for determining the dynamic undeformed chip h_d based on geometric simulation of 5-axis milling has been developed. Geometric Simulator works with Dynamic Simulator by exchanging information with it in each iteration of the simulation.

Modeling of the tool and the mass-spring-damper system

Simulating the cutting forces acting on a cutter with a complex geometry requires discretizing the cutting edges into short, approximately rectilinear elements. The generalized cutter geometry proposed by Engin and Altintas [14] is defined by seven independent parameters, marked in blue in Figure 4: D , H , α , β , R_p , r_e , λ_s . In the literature can be found several ways of

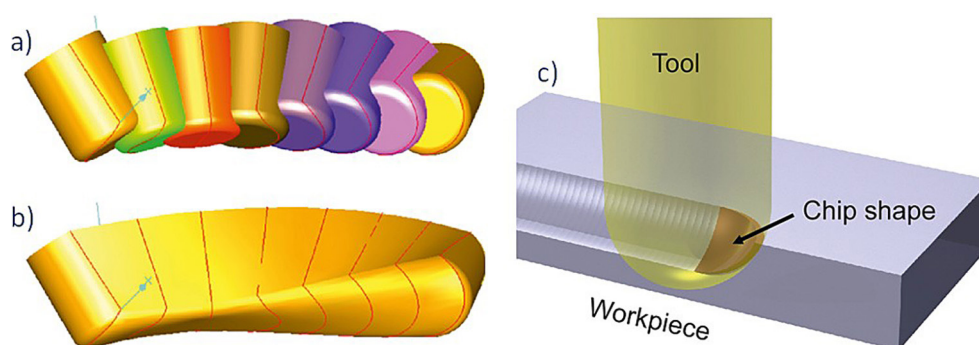


Figure 1. Discretization of the tool movement: (a) tool at different NC positions, (b) approximated sweep surface, (c) geometric model of the current chip shape based on Boolean operation [6]

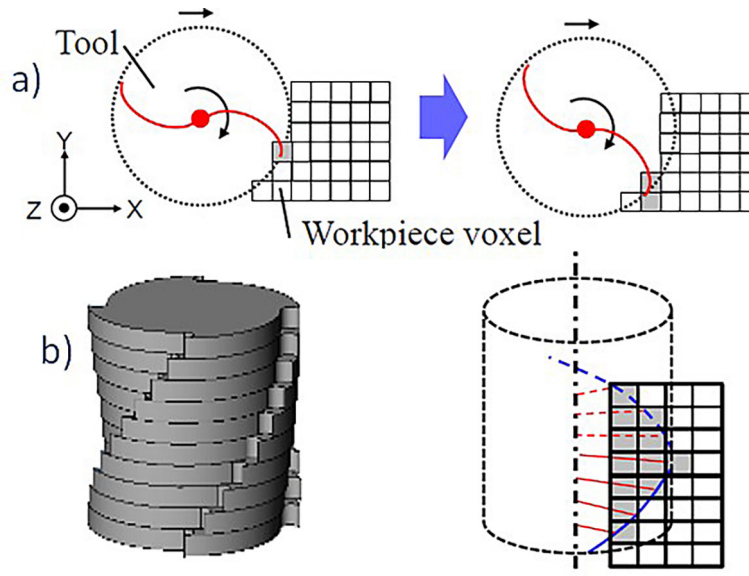


Figure 2. Extraction of removal voxels at fine tool rotation angle intervals
(a), fine disk elements comprising the cutting edge [10]

its discretization. Here the cutter is divided into narrow disks perpendicular to its Z-axis. Thus, the cutting edges are divided into segments described by parameters: the distance of the center of the segment from the cutter tip (z), the radius at which this center lies (R), the angular position of the segment center around the cutter axis (φ), the thickness of the disk (dz) and the width of the workpiece material layer cut by the segment (b). It is worth noting that b is not the length of the cutting edge corresponding to the segment – this length is l_s also shown in Figure 4. The milling machine spindle coordinate system X-Y-Z is suspended from its tip, and the Z axis coincides with the axis of the cutter. The workpiece (its material) can be represented by voxels, or octa-trees – depending on the available software.

Characteristics of the mass-spring-damper (MSD) system in milling can be modeled as a system with multiple modes in two directions

[15] as shown in Figure 5 and is represented by modal parameters: masses m_{xj} , m_{yj} , damping c_{xj} , c_{yj} , and stiffness k_{xj} , k_{yj} , where j is vibration mode number ($j=1-M$ for X axis, $j=1-N$ for Y axis). Before starting the simulation, the eigenfrequencies of all vibration modes are determined:

$$f_{0xj} = \frac{\sqrt{k_{xj}/m_{xj}}}{2\pi} \quad f_{0yj} = \frac{\sqrt{k_{yj}/m_{yj}}}{2\pi} \quad (1)$$

If the compliance of the workpiece is important, it should also be added. Here, for simplicity of description it is omitted, assuming that the workpiece is rigid. As chatter frequency is approximately equal (little lower) to one of the eigenfrequencies, to ensure the accuracy of the simulation, its frequency f_s was assumed to be ten times higher than the highest of the calculated eigenfrequencies.

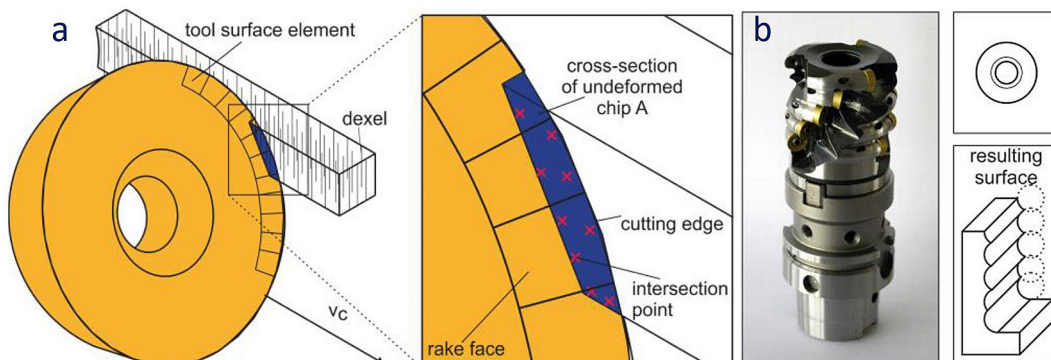


Figure 3. Tool and workpiece discretization [12, 13]

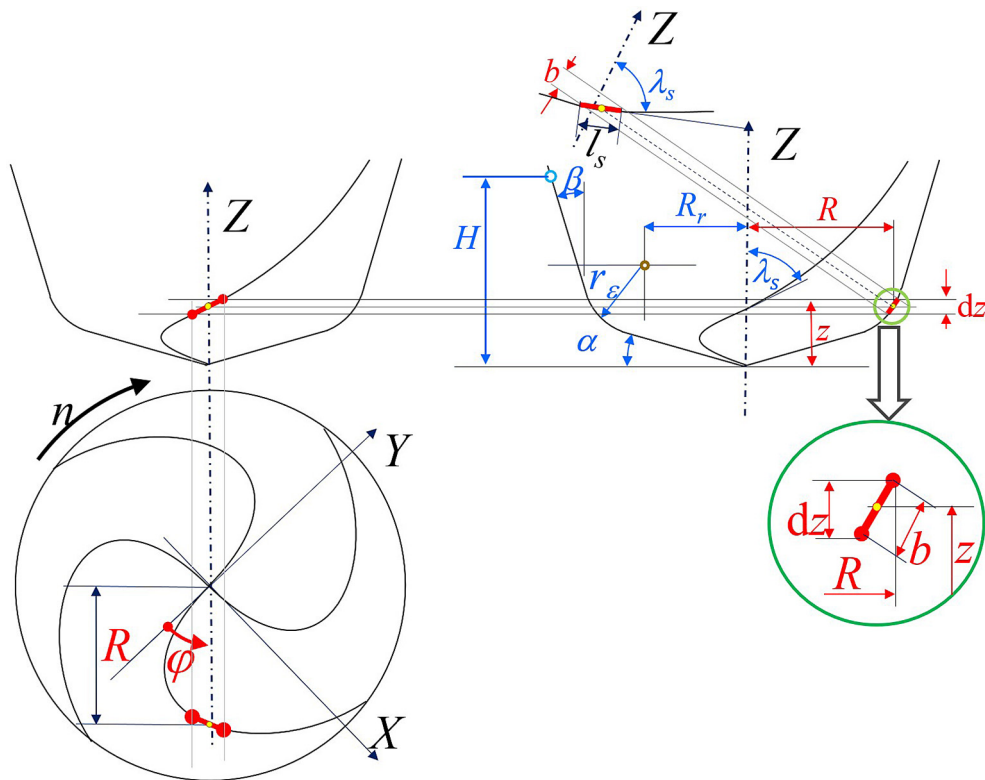


Figure 4. Discretization of universal cutter geometry into segments

Algorithm of numerical simulation of self-excited vibration

The dynamic MSD-CP system is a closed system with feedback shown in Figure 5. Simulation starts in Dynamic Simulator by calculating the instantaneous cutting forces using characteristic of CP proposed by Altintas [18] allowing the determination of the component forces from

the instantaneous section of the undeformed chip thickness:

$$\begin{aligned} F_r &= K_{rk}b + k_{rw}bh_d \\ F_t &= K_{tk}b + k_{tw}bh_d \end{aligned} \quad (2)$$

where: $K_{rk}, k_{rw}, K_{tk}, k_{tw}$ – specific cutting force coefficients.

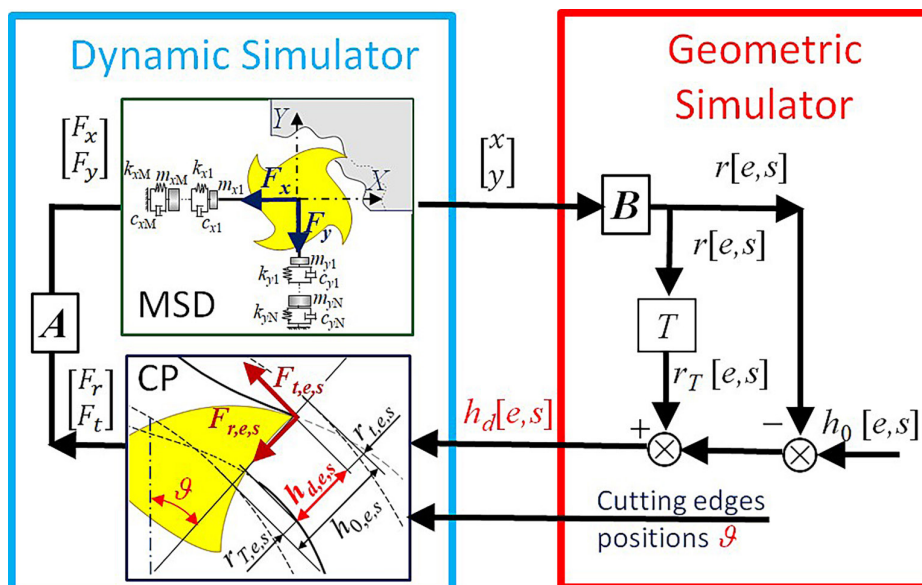


Figure 5. Dynamic machine-tool-workpiece – cutting process system

b – width of uncut chip WS,
 h_d instantaneous (dynamic) uncut chip thickness. The above formulas are applied to all segments (s) of all edges (e) involved in cutting in the current iteration giving $F_{r,e,s}$ and $F_{t,e,s}$ components, which are projected onto the X-Y reference system of the tool (transformation [A] in Figure 5) :

$$\begin{aligned} F_{x,e,s} &= -F_{r,e,s} \sin \vartheta_{e,s} - F_{t,e,s} \cos \vartheta_{e,s} \\ F_{y,e,s} &= F_{t,e,s} \sin \vartheta_{e,s} - F_{r,e,s} \cos \vartheta_{e,s} \\ F_x &= \sum_{N_e}^1 \sum_{N_s}^1 F_{x,e,s} \\ F_y &= \sum_{N_e}^1 \sum_{N_s}^1 F_{y,e,s} \end{aligned} \quad (3)$$

where: ϑ – angular position of the segment relative to the Y-axis of the milling machine spindle.

The forces F_x and F_y acting on the tool in its reference system cause vibrations in the X and Y directions. Thus, in each iteration, the Dynamic Simulator calculates accelerations, velocities, and displacements in the X and Y directions. Calculations are carried out for each mode of MSD system separately, using the force values from the previous iteration. They are based on the method proposed by Tlustý and Ismail [16]:

$$\begin{aligned} \ddot{x}_{ij} &= \frac{F_{x(i-1)} - c_{xj} \dot{x}_{(i-1)j} - k_{xj} x_{(i-1)j}}{m_{xj}} \\ \ddot{y}_{ij} &= \frac{F_{y(i-1)} - c_{yj} \dot{y}_{(i-1)j} - k_{yj} y_{(i-1)j}}{m_{yj}} \\ \dot{x}_{ij} &= \dot{x}_{(i-1)j} + \dot{x}_{ij} dt \\ \dot{y}_{ij} &= \dot{y}_{(i-1)j} + \dot{y}_{ij} dt \\ x_{ij} &= x_{(i-1)j} + \dot{x}_{ij} dt \\ y_{ij} &= y_{(i-1)j} + \dot{y}_{ij} dt \\ x_i &= \sum x_{ij} \\ y_i &= \sum y_{ij} \end{aligned} \quad (4)$$

where: i – iteration number, $dt = 1/f_s$ – iteration step.

The current vibrations in the machine spindle coordinate system – x_i, y_i are transferred to the Geometric Simulator where they are projected onto the radial direction $r_{e,s}$ for each segment s of cutting edge e each separately (transformation B in Figure 5):

$$r_{e,s} = x_i \sin \vartheta_{e,s} - y_i \cos \vartheta_{e,s} \quad (5)$$

Those radial displacements $r_{e,s}$ together with the trace left on the machined surface $r_{T,e,s}$ cause changes in the undeformed chip thickness from its nominal value h_0 to dynamic value h_d (see Figure 5). And this, in turn, results in varying cutting forces according to the equation (2)

Determination of dynamic undeformed chip thickness

In each iteration, the Geometric Simulator determines for the entire cutter the feed per tooth in the three axes f_{zX}, f_{zY} and f_{zZ} , the feed f_{zXY} , perpendicular to the cutter rotation axis, which is a vector sum (Figure 6):

$$\overrightarrow{f_{zXY}} = \overrightarrow{(f_{zX} + f_{zY})} \quad (6)$$

and the deviation of the feed from the X axis of the spindle, that is, the initial angular position of the cutter relative to the axis perpendicular to f_{XY} : ϑ_0 (Figure 6).

For all segments on all cutting edges (teeth), the Geometric Simulator determines the angular position of the segments relative to the Y axis of the machine spindle: ϑ , and relative to the axis perpendicular to the feed f_{zXY} : Ψ . This allows to determine the nominal feed of the segment in the radial direction between the passes of successive teeth in the reference plane Pr of the segment:

$$f_{rZ} = f_{zXY} \sin \Psi \quad (7)$$

The nominal position of the edge segment in the plane perpendicular to the cutter axis is superimposed on the displacements of the entire cutter (x and y) determined by the Dynamic Simulator, which, when projected in the radial direction, give the displacement in that direction:

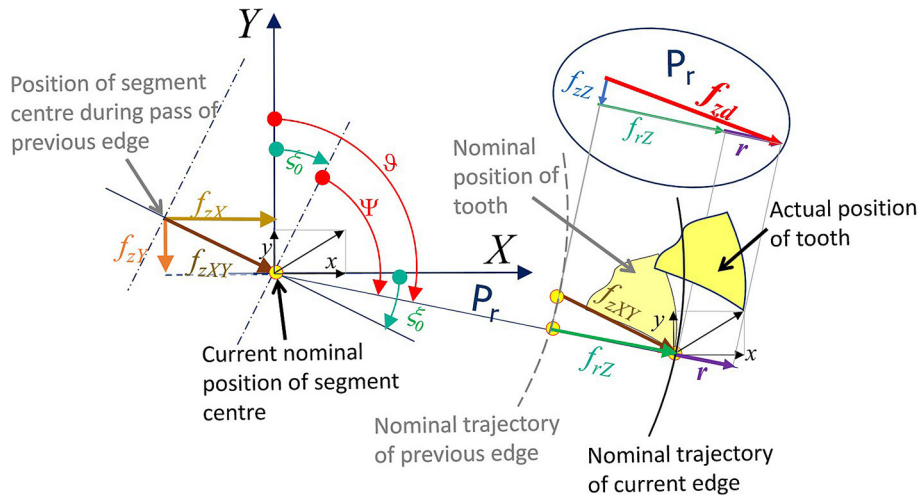


Figure 6. Determination of dynamic feed per tooth

$$r = x \sin \vartheta - y \cos \vartheta \quad (8)$$

Considering the feed per tooth in the Z-axis direction $-f_{zz}$ – the dynamic feed f_{zd} can be determined:

$$f_{zd} = f_r + r = f_{zXY} \sin \Psi + r \quad (9)$$

This makes it possible to determine the current position of the center of the segment (point A in Figure 7), taking into consideration both nominal movements and vibrations of the tool relative to the workpiece, and subtracting the material (voxels) removed by the segment from the workpiece. This creates a cut surface formed

by the tooth passage, considering vibrations. The Geometric Simulator then determines a point (B in the figure), on the outer surface of the uncut chip lying on a straight line drawn from the center of the segment (point A) along the vector \vec{f}_{zd} . The outer surface of the uncut chip can be the surface formed by the passage of the previous tooth, taking into consideration vibrations, or the outer surface of the workpiece or the further point of the cutting edge. This makes it possible to determine the distance of the center of the segment from the outer surface of the uncut chip along the vector \vec{f}_{zd} (the length of the segment A-B in the Figure 7), and to calculate the dynamic thickness of uncut chip h_d which is the projection of the segment A-B in the direction perpendicular to the tangent to the cutting edge.

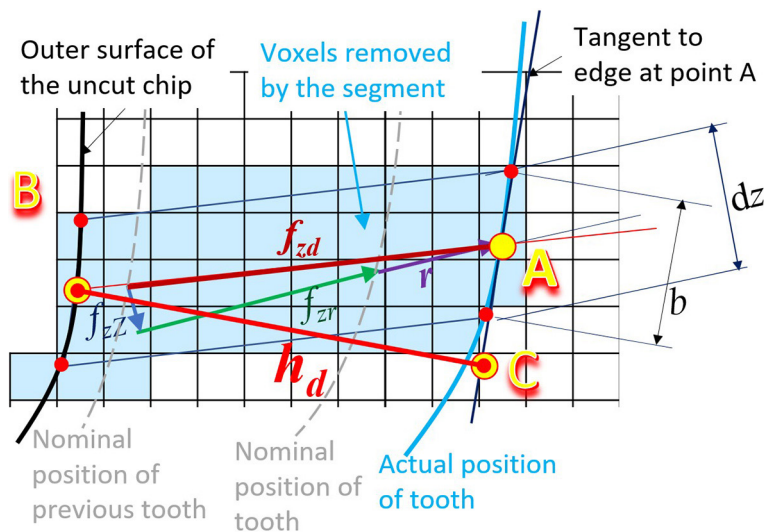


Figure 7. Determination of actual undeformed chip thickness h_d

The result of the Geometric Simulator passed to the next iteration is (for all cutting edges and segments) a 2D array of dynamic thicknesses of the uncut chip h_d [edge, segment]. This allows the Dynamic Simulator to determine the cutting forces acting on the cutter and simulate the displacement (vibration) of the cutter in the X and Y directions then passed to the Geometric Simulator. The flow of data in each iteration is shown in Figure 8.

Effect of voxel dimension on the accuracy of simulation of self-excited vibrations

Numerical simulation is inherently discrete in time (simulation step d $dt=1/f_s$). The use of geometric simulation, in which the material is represented by discrete voxels, further introduces signal quantization, that is, limited resolution of uncut chip thickness h_d and trace left by previous tooth on the machined surface r_r . The voxel size determines the grid resolution, simulation performance and calculation accuracy – a smaller voxel size leads to higher resolution, higher memory consumption and longer calculation time, and vice versa – a larger size means lower resolution, lower memory consumption and shorter calculation time. Therefore, it is important to select the largest possible voxel size that allows satisfactory accuracy of simulation of self-excited vibrations. To make a preliminary estimate of the effect of voxel size on simulation accuracy, simulation experiments were conducted using end mill TIZ UFX11–20, D=20mm, 4 flutes, $\lambda_s=30^\circ$. Modal parameters of MSD system and frequency response function for X axis (FRF for Y axis is

similar) obtained experimentally by tap tests, are presented in Table 1.

Workpiece material: steel C45, cutting force coefficients obtained experimentally by full slot milling: $K_{rk}=27$ N/mm, $k_{rw}=788$ N/mm², $K_{tk}=198$ N/mm, $k_{tw}=1319$ N/mm². Cutting conditions: $a_e=3$ mm, $a_p=3$ mm, $f_{zX}=50\mu\text{m/tooth}$, $f_{zY}=0$, $f_{zY}=0$, $n=3000$ rev/min, down milling. Simulation frequency was 20 kHz, which gives 400 iterations/revolution.

Examples of test results are presented in Figure 9. For the beginning, a very small voxel size of 1 μm was taken – Figure 10a. As can be seen in the waveform graph above, within two rotations of the cutter, self-excited vibrations developed. The bottom graph shows uncut chip thickness h_d at one segment – due to partial immersion of the cutter it covers only 50 iterations. The next simulation was performed for the voxels size equal to half of feed per tooth: 25 μm . It resulted in quantization of h_d to three levels – 0, 25 and 50 μm (Figure 10b). Apart from the first 50 iterations, the vibration waveform has hardly changed. Application of a voxel size equal to the feed per tooth: 50 μm – Figure 10c resulted in a radical quantization of h_d to only two levels – 0 and 50 μm . Nevertheless, the course of vibrations, which are calculated by the Dynamic Simulator without quantization, has changed slightly. However, further increasing the dimension of the voxels leads to a significant deterioration in simulation accuracy, as can be seen in Figure 10d, where voxel size of 70 μm was applied.

These results indicate that although higher resolution is beneficial for more accurate prediction of vibration waveforms, very high resolution

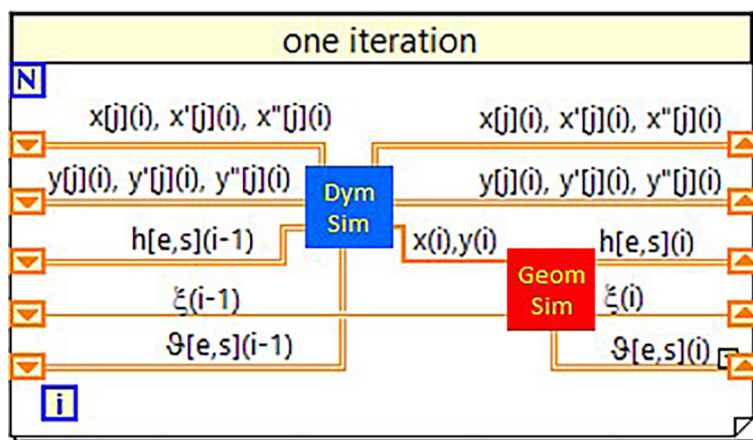


Figure 8. Data flow between dynamic and geometric simulator in each iteration

Table 1. Modal parameters of mass-spring-damper system applied in simulations

m_{xj} (kg)	c_{xj} (Ns/m)	k_{xj} (N/m)	m_{yj} (kg)	c_{yj} (Ns/m)	k_{yj} (N/m)
0.204	0.150	2.17E+4	0.165	0.150	1.81E+4
0.172	0.191	4.21E+4	0.160	0.202	4.12E+4
1.800	0.794	5.99E+5	0.519	0.270	3.14E+5

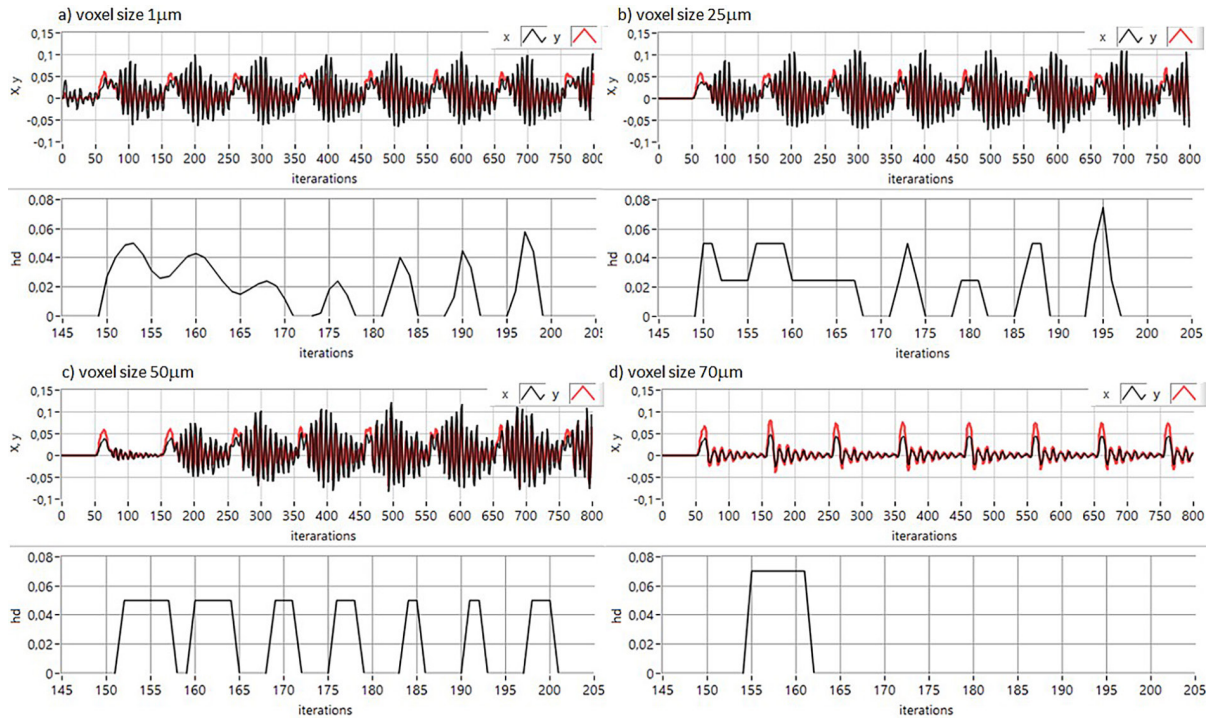


Figure 9. Simulation accuracy dependence on voxel size

(small voxel size) is not necessary for simulating self-excited vibrations

CONCLUSIONS

This study developed a novel simulator of self-excited vibrations in 5-axis milling, in which geometric simulations defining nominal milling movements were integrated with dynamic simulations. Simulation procedures were divided into two modules. Dynamic Simulator calculates cutting forces and MSD system vibration in the milling machine spindle coordinate system XY. Geometric Simulator uses computer graphics for determination of nominal position of every cutting edge segment and its engagement in workpiece material. Adding the vibrations of the tool relative to the workpiece determined by the Dynamic Simulator allows the Geometric Simulator to consider these vibrations to determine the dynamic uncut chip thickness and the trace left by the tooth

on the material surface. This trace is taken into consideration for determining the dynamic chip thickness when the next tooth passes through the same area of the workpiece. The effect of voxel size on the accuracy of vibration simulation is also presented.

Acknowledgements

Financial support of Operational Programme Smart Growth – Project “CYBERTECH 4 – a system for intelligent design of the technological process for the 4.0 platform”, No POIR.01.01.01–00–0547/20 is gratefully acknowledged.

This publication was financed from the funds of the Ministry of Education and Science as part of the program Social Responsibility of Science / Excellent Science Name and module of the application: Excellent Science – Support for Scientific Conferences Synergy of Science and Industry, Challenges of the 21st Century, Science – Industry – Business

REFERENCES

1. Zhu L., Liu C. Recent progress of chatter prediction, detection and suppression in milling. *Mechanical Systems and Signal Processing* 2020; 143: 106840.
2. Altintas Y., Stepan G., Budak E., Schmitz T., Kilic Z. M. Chatter Stability of Machining Operations. *Journal of Manufacturing Science and Engineering* 2020; 142(11): 110801.
3. Munoa J., Beudaert X., Dombovari Z., Altintas Y., Budak E., Brecher C., Stepan G. Chatter suppression techniques in metal cutting. *CIRP Annals – Manufacturing Technology* 2016; 65(2): 785–808.
4. Båk P.A., Jemielniak K. Self-excited vibrations avoidance methodology in non-linear numerical simulation environment. *Procedia CIRP* 2017; 62: 245–249.
5. Jemielniak K., Widota A. Numerical simulation of non-linear chatter vibration in turning, I *International Journal of Machine Tools and Manufacture* 1989; 29: 239–247.
6. Altintas Y., Kersting P., Biermann D., Budak E., Denkena B., Lazoglu I. Virtual process systems for part machining operations, *CIRP Annals-Manufacturing Technology* 2014; 63: 585–605.
7. Yang Y., Zhang W., Wan M., Ma Y. A solid trimming method to extract cutter–workpiece engagement maps for multi-axis milling, *The International Journal of Advanced Manufacturing Technology* 2013; 68: 2801–2813.
8. Yousefian O., Balabokhin A., Tarbuton J. Point-by-point prediction of cutting force in 3-axis CNC milling machines through voxel framework in digital manufacturing. *Journal of Intelligent Manufacturing* 2020; 31: 215–226.
9. Xi X., Cai Y., Wang H., Zhao D. A prediction model of the cutting force–induced deformation while considering the removed material impact. *The International Journal of Advanced Manufacturing Technology* 2022; 119: 1579–1594.
10. Nishida I., Okumura, Sato R., Shirase K. Cutting Force and Finish Surface Simulation of End Milling Operation in Consideration of Static Tool Deflection by Using Voxel Model. *Procedia CIRP* 2018; 77: 574–577.
11. Li J., Kilic Z.M., Altintas Y. General Cutting Dynamics Model for Five-Axis Ball-End Milling Operations. *ASME. J. Manuf. Sci. Eng.* 2020; 142(12): 121003.
12. Denkena B., Grove T., Pape O. Optimization of complex cutting tools using a multi-dexel based material removal simulation. *Procedia CIRP* 2019; 82: 379–382.
13. Denkena B., Pape O., Krödel A., Böß V., Ellersiek L., Mücke A. Process design for 5-axis ball end milling using a real-time capable dynamic material removal simulation. *Production Engineering* 2021; 15: 89–95.
14. Engin S., Altintas Y. Generalized modeling of milling mechanics and dynamics: Part I–Helical end mills. *American Society of Mechanical Engineers Manufacturing Engineering Division MED* 1997; 10345: 352.
15. Zhu L., Liu C. Recent progress of chatter prediction, detection and suppression in milling. *Mechanical Systems and Signal Processing* 2020; 143: 106840.
16. Tlustý J., Ismail F. Basic Non-linearity in Machining Chatter. *CIRP Annals – Manufacturing Technology*, 1981; 30: 21–25.
17. Tunc L.T., Mohammadi Y., Budak E. Destabilizing effect of low frequency modes on process damped stability of multi-mode milling systems. *Mechanical Systems and Signal Processing* 2018; 111: 423–441.
18. Altintas Y. *Manufacturing automation: Metal cutting mechanics machine tool vibrations and CNC design*. Cambridge University Press, 2012.